CAV2021
11th International Symposium on Cavitation
May 10-13, 2021, Daejon, Korea

Valve-like Torus-margo Pit of Gymnosperms Regulating Spread of Cavitation

Jooyoung Park [1]*, Sung Ho Park [2], Jeongeun Ryu and Sang JoonLee [1]*

[1]Department of Mechanical Engineering, POSTECH, Pohang, 37673, Republic of Korea

Abstract: Gymnosperms widespread in arid climate have survived against vulnerability of cavitation in xylem trachieds. Torus-margo (TM) pit has been reported as a crucial structure which enables safe water-transport by controlling embolism spread through adjacent xylem conduits. However, detailed hydrodynamics of TM pit remains unclear even at a single pit-level. In this study, we investigated the hydraulic roles of a single TM structure in terms of prevention of cavitation spread by using a synthetic TM-pit system. As a result, TM structure was found to lead a tight overlap of torus structure with the aperture and enhance the resistance against both initial and consecutive air spread without losing hydraulic conductivity. Our experimental results indicate that TM-pit of gymnosperms may moderate the trade-off between hydraulic safety and efficiency of sap transport with their special valve-like motion. The present study would advance our understanding of survival strategy of gymnosperms from the pit-level living harsh environments where cavitation frequently occurs.

Keywords: cavitation resistance, hydraulic conductivity, torus-margo pit, plant hydrodynamics

1. Introduction

Cavitation usually occurs inside xylem conduits of plants since they using a suction pressure to transport water [1]. Gymnosperms, living in arid region, have been known to develop unique structures "torus-margo (TM) bordered pits" to ensure safe and efficient water transport at the risk of cavitation. Boredred pits contains a pit membrane composed of a thickened torus (violet-colored regions in Fig. 1(a)) at the center and a highly porous margo at the toroidal region. The TM pit membrane is enclosed in the middle of a pit chamber, having a couple of pit apertures facing each other where fluids can flow through.

In spite of much interest in TM pits, the exact hydraulic mechanism of spread of cavitation bubbles through them still remains unclear. Hydraulic conductivity and the pressure required for air-spreads through a single pit were estimated indirectly from the cut stems containing multiple pits connected in parallel. Morphological characteristics of the TM pit were proposed to minimize the spread of cavitation or moderate the safety-versus-efficiency tradeoff from an evolutionary point of view, but which are also in debate [2]. The direct experimental studies on the interfacial phenomena in a single TM pit of real plants are in fact technically limited because the micro-scale pit structures are embedded at the complicatedly interconnected flow channels.

In this paper, we study the valve-like dynamics to regulate two-phase flows through the TM pit considering the effect of fluid-structure interactions. Using synthetic TM bordered-pit models, we present systematic experiments of the air spreading dynamics and the fluid flow characteristics at the single pit level. It shows the initial onset and the consecutive continuous and discontinuous air-spreads, and the flow characteristics in the TM-pit models. Based on the experimental results, we propose the structural criteria of the TM pits to prevent both air-spreading stages and discuss them with botanical data in the viewpoint of the safety-versus-efficiency tradeoff.

* Corresponding Author: Sang Joon Lee, sjlee2169@postsech.ac.kr

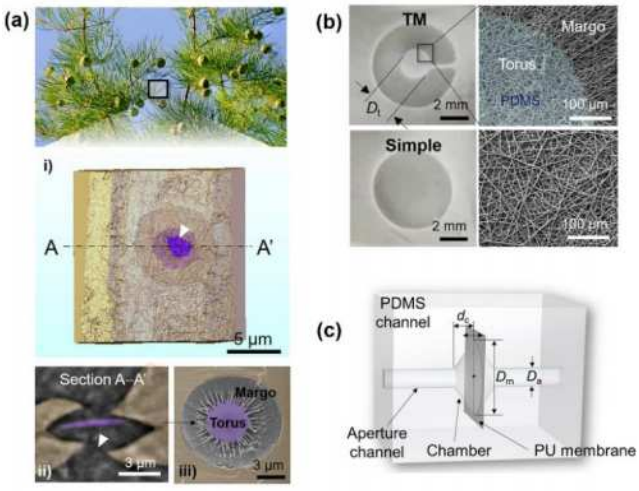

Figure 1. Characteristics of bordered-pits of *Taxodium distichum* and soft pit valve models. (a-i) 3D microscopic images of a torus-margo (TM) pit of *Taxodium distichum*. (a-ii) Reconstructed X-ray image of the TM pit corresponding to the cross-section A—A′. White arrowheads indicate pit apertures. (a-iii) Scanning electron microscopy (SEM) images of TM pit membrane. (b) A synthetic soft pit valve membranes and their SEM images. (c) The bordered-pit model system comprising a pair of chamber structures embedding a PU membrane unit.

2. Materials and Methods

2.1. Fabrication of synthetic bordered-pit models

For the synthetic bordered-pits used in the experiments, polyurethane (PU) membranes were fabricated by the electrospinning technique (Fig. 1(b)). PU fibers were deposited to make homogeneous circular membranes for both of TM- and simple-type bordered-pit models. To mimic the torus structure, PU fibers were overstacked on the circular region with the diameter (D_t) of 2 mm in the middle of the TM-type membrane, and covered with a 10:1 wt% mixture of polydimethylsiloxane (PDMS) and curing agent (Sylgard-184, Dow Corning). We made 4 different membranes having different morphologies for each bordered-pit system by controlling the electrospinning time in 10, 20, 30, and 40 min. Each simple membrane, which was fabricated during the same spinning time with that of the TM membrane, has similar morphology with that of the margo region of the TM membrane. Membrane morphologies such as membrane thickness, average and maximum pore size, and porosities are characterized by SEM images and X-ray imaging. Those TM and simple membranes sharing morphological features were grouped by average thickness l_{avg} which was obtained by averaging the thickness of the simple membrane and the margo region of the TM membrane. A piece of PU membrane was sandwiched between a couple of chamber structures (made of PDMS) facing each other and combined as a bordered-pit system (Fig. 1(c)).

2.2. Working fluid and flow conditions

To observe the air spreading dynamics through the wetted membrane structures, we chose Krytox 103 oil (Miller-stephenson Chemical Co.) as the working fluid for the synthetic bordered-pit models. PU membrane is hydrophobic (water contact angle ≈ 133.0°, oil contact angle ≈ 16.6°), into which the oil can easily permeate. The density, surface tension, and viscosity of the oil are, respectively, ρ =1900 kg/m3, γ =17.7 mN/m, and μ=80 cSt. To achieve dynamic similarity with real sap flows [1], Reynolds number and capillary number were adjusted to range within 10^{-1}–10^{-2} and 10^{-3}, respectively. Air spreading behaviors and membrane deflection were monitored by X-ray imaging at 6C beamline at Pohang Accelerator Laboratory (PAL; Pohang, Korea) under the same experimental conditions of our previous work [3]. During the experiment, pressure variations at the downstream of the synthetic pit-model was measured with a pressure transducer (PX409-015GUSB, Omega Engineering).

* Corresponding Author: Sang Joon Lee, sjlee2169@postsech.ac.kr

3. Results

3.1. Onset of air penetrationi through the synthetic TM-pit model

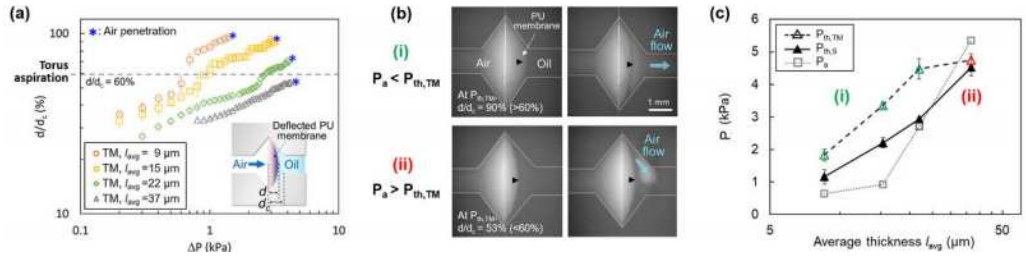

Figure 2. Onset of air penetration through the synthetic TM-pit model. (a) Membrane deflection d relative to the chamber depth d_c (inset) with ΔP across the TM-pit systems. (b) (b-i) Air penetration when $P_a < P_{th,TM}$ and (b-ii) $P_a > P_{th,TM}$. (c) Threshold pressure of TM- ($P_{th,TM}$) and simple-pit system ($P_{th,S}$).

We observed the onset of air penetration with the deflection of the fully wetted TM membranes d (inset of Fig. 2(a)) by monitoring the pressure difference ΔP across the membrane (Fig. 2(a)). Since reaching $d/d_c \approx 60\%$, where d_c is a chamber depth, a margo region contacts with the chamber walls and the torus structure seals the aperture channel, which is called '(torus) aspiration'. The thin three TM-membranes show the onset of air penetration at the threshold pressure P_{th} (blue asterisks) after the aspiration at P_a. The air penetrates through the thin membranes at $P_{th} > P_a$ (Fig. 2(b-i)). By contrast, the thickest membrane shows the air spread before the aspiration. P_a of the thickest TM membrane is estimated to be higher than its P_{th}. When $P_a < P_{th}$, P_{th} of TM-pit ($P_{th,TM}$) is higher than that of simple-pit $P_{th,S}$ having the same average thickness (Fig. 2(c)). By contrast, $P_{th,TM}$ is comparable with $P_{th,S}$ when $P_a > P_{th}$. In this case, the torus region is unable to seal the aperture channel and air penetrates through the margo region. This results indicatse that the TM-pit system with thin membranes increases P_{th} and delay the onset of air penetration by torus aspiration.

3.2. Consecutive air-spread through the synthetic TM-pit model

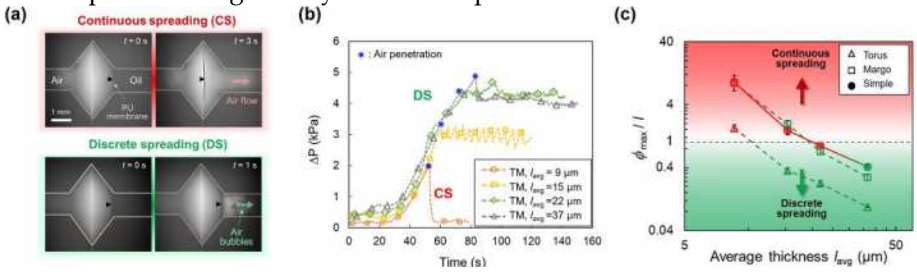

Figure 3. Consecutive air-spread through the TM-pit model. (a) Two types of air-spread: continuous spread (CS) and discrete spread (DS). (b) Temporal variations of ΔP across the TM-pit models. (c) Two types of air spreading classified by the ratio of the maximum pore size ϕ_{max} to the membrane thickenss l.

We observe two modes of air-spreading after the onset of air penetration: continuous and discrete spreading (CS and DS, respectively) (Fig. 3(a)). In CS, air continuously spread across the TM-pit model and the membrane returns to its original position. ΔP is immediately released to $\Delta P \approx 0$ after the air penetration (blue asterisks). However, for DS, air discontinuously spreads forming air bubbles, and the membrane remains to be deflected. During DS, ΔP fluctuates around P_{th} due to the repetition of the break and recovery of the oil film near the membrane. All TM-type membranes exhibited DS except the thinnest membrane.

We compare TM-pit to simple-pit models by evaluating the ratio between the largest pore diameter ϕ_{max} to the membrane thickness l (Fig.3(c)), similarly to the case of wetted cellulose membranes [3]. The simple-pit models having l_{avg} of 9, 15, 22 μm, have $\phi_{max}/l_{avg} > 1$ and exhibit CS, while the simple-pit with the

* Corresponding Author: Sang Joon Lee, sjlee2169@postsech.ac.kr

thickest membrane (l_{avg}=37 μm, ϕ_{max}/l_{avg} <1) exhibit DS corresponding to our previous model [3]; the surface energy can be lowered when the liquid film inside the pore is withdrawn, showing CS when $\phi_{max} > l$.

3.3. Hydraulic function of the TM pits in plants in terms of safety and efficiency

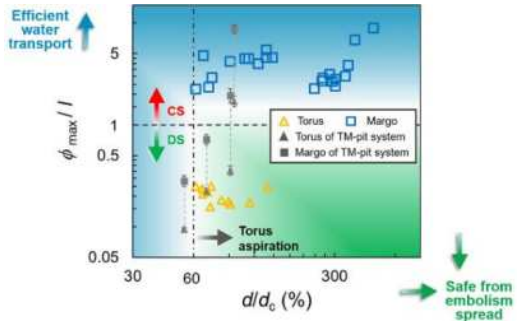

Figure 4. Safety and efficiency map of the torus [4] and margo [5] structures of real plant species.

Based on our experimental results, we examined the hydraulic roles of TM pits in real plant species in the terms of the prevention of embolism spread and its tradeoff with the water transport efficiency (Fig. 4). We obtained d/d_c of the TM pits at P_{th} by using to the following equation,

$$d/d_c = 0.24\, l/d_c\, (\Delta P D_m^4/El^4)^{1/3}. \quad (1)$$

Here, the elastic modulus E of the margo part is used to be 3 GPa, as suggested in a previous study, and the thickness of the margo strands is used for l. Figure 4 shows that the ϕ_{max}/l values tori and margo strands from botanical data are located on the upper and lower sides of the dashed-horizontal line ϕ_{max}/l=1, respectively, and enables the air spread through the TM pits to be DS. Thus, the TM pits have benefits to safe transport against the further embolism spread as well as the onset of the air penetration, by having the more impermeable structure, the torus, than the margo, without losing hydraulic conductivity.

The geometric scale of the synthetic bordered-pit systems were not exactly same as those of real plants. However, deformability of the pit membranes and their chemical affinity with water were favorably reflected in our study. The present results are still meaningful to provide new insights into the safety roles of TM-pit membranes in preventing embolism spread at the pit level.

Acknowledgments: We thank Dr. J. Lim and Dr. S. Lee at the 6C and 7C beam lines of Pohang accelerator laboratory (PAL) for supporting the X-ray imaging experiments.

References

1. Jensen, K.H., Berg-Sorensen, K., Bruus, H., Holbrook, N.M., Liesche, J., Schulz, A., et al. Sap flow and sugar transport in plants. *Rev. Mod. Phys.* **2016**, *88(3)*, 035007.
2. Delzon, S., Douthe, C., Sala, A. & Cochard, H. Mechanism of water-stress induced cavitation in conifers: bordered pit structure and function support the hypothesis of seal capillary-seeding. *Plant Cell Environ.* **2010**, *33*, 2101-2111.
3. Park, J., Go, T., Ryu, J. & Lee, S.J. Air spreading through wetted cellulose membranes: implications for the safety function of hydraulic valves in plants. *Phys. Rev. E* **2019**, *100*, 032409.
4. Jansen, S., Lamy, J.B., Burlett, R., Cochard, H., Gasson, P., and Delzon, S., Plasmodesmatal pores in the torus of bordered pitmembranes affect cavitation resistance of conifer xylem. *Plant Cell Environ.* **2012**, 35, 1109-1120.
5. Domec, J.C., Lachembruch, B., and Meinzer, F.C., Bordered pit structure and function determine spatial patterns of air-seeding thresholds in xylem of Douglas-fir (*Pseudotsuga menziesii*; Pinaceae) trees, *Am. J. Bot*. **2006**, *93(11)*, 1588-1600.

* Corresponding Author: Sang Joon Lee, sjlee2169@postsech.ac.kr